INSTITUTE OF HIGH ENERGY PHYSICS, SERPUKHOV

Report IFVE SEF 71-89

SELECTION OF ELECTRONS IN SECONDARY PARTICLE BEAMS OF UP TO 50 GeV/c AND DETECTION OF ELECTRON SHOWERS

V.A. Kachanov, V.M. Kut'in, V.G. Lapshin,
V.I. Rykalin and V.K. Semenov

Serpukhov 1971

Translated at CERN by R. Luther
(Original: Russian)
Not revised by the Translation Service

(CERN Trans. 72-9)

Geneva
May 1972

Introduction

Among the physical experiments being carried out at the IHEP accelerator, high-energy electrons (positrons) or γ -quanta are being detected as the end product of reactions. It is necessary to adjust and calibrate the detection equipment at various electron beam energies and to measure the energy resolution of the electron and γ -quantum detectors. At the IHEP, pure electron beams may be obtained in the neutral $1K^{o}$ [1] channel, yet the number of electrons per cycle at 15 GeV/c is low. Moreover, it is not always convenient to move the device (or a part thereof) to another channel. At the same time, the results given in papers [2,3] indicate that secondary beams contain a sufficient electron admixture for a number of systematic investigations. This raises problems concerning not only the detection of the electrons in the secondary particle beams [3], but also their selection for systematic or physical investigations.

This report describes the application of high-resolution threshold Cerenkov counters [4] for the selection of electron beams of up to 50 GeV/c and gives data on electron yields as well as the results of some systematic investigations on electron beams. The results of electron energy measurements using lead-scintillation sandwiches are given, as are the transverse dimensions of electron showers using a scintillation hodoscope based on a hodoscopic photomultiplier [5].

1. Detection of electrons using threshold Cerenkov counters

The measurements were carried out in the 4A magneto-optical channel [1]. The electrons were detected by means of two threshold Cerenkov counters $\check{C}_1$ and $\check{C}_2$ [4] with an overall length of approximately 30 m. The beta resolution of each counter was $\delta\beta \approx 5.10^{-6}$. The counters were connected in coincidence with a scintillation telescope M (5 scintillation counters placed along the channel). Fig.1 shows a typical threshold curve at 25 GeV/c.

As can be seen from the figure, the threshold counter system detects electrons below the μ^--meson detection threshold and the electron content in the beam is $1{,}4 \cdot 10^{-2}$. The efficiency of the Cerenkov counters below the μ^--meson detection threshold was determined from the calibrated threshold curve, measured for π^--mesons.

It should be pointed out that the use of threshold beta discrimination for electron detection is not always justified as the number of random pulse coincidences from noise and background loading of the counter's photomultiplier with beam particles may in this case be compared with the number of electrons in the beam.

In order to determine the purity of the electron beam selected, we used lead-scintillation sandwiches. One of them consisted of five scintillators measuring 150 x 100 x 10 mm^3 sandwiched between lead plates 5 mm thick (2,5 cm of Pb altogether) and was used to measure the electron energy in terms of the energy release in the region of the shower curve's maximum. Light from the scintillators was collected by means of a plexiglass light-guide attached to an FEU-30 photomultiplier. The other sandwich was a total absorption counter consisting of 20 scintillation plates 150 x 150 x 10 mm^3 sandwiched between lead plates 10 cm thick overall. Light was collected by means of a hollow light-guide with aluminized mylar walls attached to an FEU-49 photomultiplier. Figs. 2a and 2b show typical spectra obtained when detecting electrons by means of the sandwiches. The results show that the admixture of other particles in the electron beam selected does not exceed 15% at 25 GeV/c. As the momentum increases, the purity of electron selection worsens somewhat: this is connected first of all with the lower electron content in the beam and secondly with a poorer electron detection efficiency $\varepsilon(E) \sim 1/E^2$. However, this form of selection is quite adequate for a number of practical purposes. Clearly, the purity of beam selection may be improved by increasing the number of threshold Cerenkov counters connected in coincidence.

Electron yields may be measured more directly if the number of counts in the electron peak of the sandwich's pulse-height spectrum is recorded at various gas pressures in the threshold counter. This technique has advantages when moving into the high-energy part of the spectrum $E > 40$ GeV as the threshold curve for the electrons can be traced over a wider pressure range beyond the μ-meson and π-meson detection threshold. Fig.3 shows the dependence of the count in the electron peak on the pressure in the counters. Data on the electron content in the beam were also obtained by analyzing the pulse-height spectra from beam particles using the total absorption counter (Fig.4) without the threshold counters.

The electron yield values obtained by the various methods $R = N^{e^-}/N_{\pi^-}$ coincided and are given in table 1*.

Table 1

Al target, 20 mm. long, particles' angle of extraction into the channel $\theta = 0$

p GeV/c	25	32,5	40	48
$R \cdot 10^{-3}$	14	3,7	1,1	0,8

2. Measurement of electron energy by means of lead-scintillation sandwiches

There are two main known methods for measuring electron and γ-quantum energy using sandwiches - in terms of the energy release in the region of the shower's maximum /6/ and in terms of the total energy release when using total absorption sandwiches. An extremely simple way of applying the first method is to use sandwich hodoscopes,

* The measurement error is $\pm$ 20%.

by means of which the energy and coordinates of several simultaneous electrons or γ-quanta can be measured. However, the energy resolution of the sandwiches [6] is considerably worse than the resolution of total absorption sandwiches [7,8] in the previously investigated energy range up to 10 GeV.

We made comparative measurements of the energy resolution using a total absorption sandwich (10 cm Pb, 20 layers) and a sandwich at the maximum of the shower curve (2,5 cm. Pb 5 layers) over the momentum range 2,5 - 50 GeV/c. Measurements in the 2,5 - 14 GeV/c region were carried out in the 1K° channel. The system for selecting the electron beam (Fig.5) is similar to that used in paper [6]. For selected momentum values in the region up to 20 GeV/c, the shower curves were measured using the "sandwich" (2,5 cm. Pb) and mean values for the sandwich's pulse-height spectra were found corresponding to the maxima of the shower curves. For momenta of 32,5 GeV/c and 40 GeV/c, it was assumed that the shower curve maxima were reached with an overall lead thickness of 5,5 cm.

Figures 6a and 6b show the dependences of the energy resolution and the mean values of the sandwich's pulse-height spectra on the momentum value. The linearity and energy resolution of the total absorption sandwich in the momentum range up to 50 GeV/c are shown in Fig.7. Typical pulse-height spectra of the sandwiches at various momenta are given in Figs. 2a and 2b. The data in Fig.6b show that the energy resolution for the sandwich (2,5 cm. Pb) is $2\gamma \sim E^{-1/2}$, where E is the electron's energy.

The linear dependence on momentum of the mean pulse-height in the sandwich (2,5 cm. Pb) is in agreement, within the limits of measurement error, with the theoretical energy dependence [9] of the number of particles at the shower's maximum (viz. Fig.6a):

$$\bar{N}_{max} \sim (E_o/\varepsilon_o)\ (\ell n\ E_o/\varepsilon_o)^{-1/2} \quad (I),$$

where E_o is the energy of the primary γ-quanta or electrons and ε_o is the critical energy.

In the case of the total absorption sandwich, the energy resolution reaches a plateau at E = 15 GeV. In order to explain the reason for this, we studied rate effects on the sandwich with beam particles and measured the energy spectrum of the part of the electromagnetic shower escaping from the counter. It turned out that the rate did not affect the resolution and the relative fluctuations of the escaping part of the shower with respect to the mean pulse-height from the sandwich at P = 32,5 GeV/c were less than $\pm$ 1,5%. The sandwich's intrinsic resolution when the photocathode was lit by light pulses from the light diode (the mean values of the pulse heights from the electrons at P = 32,5 GeV/c and the light pulses from the light diode coincided) was $2\tau \simeq 2\%$.

The following reasons may be put forward for a plateau in the energy resolution:

1. Only one photomultiplier was used in the total absorption sandwich, which, with a beam cross-section of 50 mm., could lead to a considerable dependence of light collection on the position of the primary electron's trajectory relative to the photomultiplier's photocathode.

2. The photocathode's sensitivity in the radial direction dropped 1,5 times from the mean radius ($0,5\ r_{max.}$) to the edge of the photocathode ($r_{max.}$). Therefore, the shower's longitudinal fluctuations may lead to a re-distribution of the energy release in the various scintillators of the sandwich and consequently to a worsening of the energy resolution.

III. Definition of the transverse dimensions of the electron showers

As a rule, the data published on the transverse dimensions of electron showers relate to the development of showers in solid

media (Cu, Pb etc.). However, a number of experiments require data on the dimensions of electromagnetic showers developing in laminar media - sandwiches, which consist, for example, of scintillators or gas-discharge chambers sandwiched between lead plates.

In order to define the dimensions of the electron showers, we used a scintillation hodoscope based on a hodoscopic photomultiplier /5/. The hodoscope consisted of 15 scintillation rods 150 x 10 x 5 mm^3, the ends of which made optical contact with the surface of the photocathode. The distance between the rods along the photocathode was 7 mm. The overall dimensions of the hodoscope's sensitive volume were 150 x 100 x 10 mm^3 (10 mm. in the beam direction).

The transverse dimensions of the showers were measured at varying thicknesses of the lead in front of the hodoscope and also using laminar media. A scintillation counter was placed in front of the hodoscope to determine the dimensions of the electron beam detected. The scintillator measured 50 x 10 x 2 mm^3 (10 mm. along the beam and 50 mm. along the plane of the hodoscope's scintillators). Pulses from the hodoscope were fed to the input of a 5-beam oscilloscope and photographed.

Depending on the number of particles passing through the hodoscope's scintillators, their corresponding FEU current pulses will vary in height and will be staggered in time. A typical oscillogram of hodoscope pulses is shown in Fig.8. The position of the pulse tops corresponding to the different scintillators can be distinguished fairly clearly. It is obvious that the transverse dimensions of the showers may be defined from the results of the oscillograms, with the necessary corrections.

The pulse-height and time calibration of the hodoscope was done when particles were detected (without lead). In the case of the pulse-height calibration, the pulse-height distribution was

produced for each scintillator and the mean pulse-height value was found. It turned out that the mean pulse-heights from the various scintillators did not differ by more than $\pm$ 6% over the working range.

The time calibration was done by moving the hodoscope across the beam. The spread of the differences in delay time for the output pulses as particles passed through the adjacent scintillators did not exceed $\pm$ 10%.

With the showers measured, it is desirable to place the detector directly behind the lead due to the presence of a finite angular divergence of the particles in the shower. In our case, it was impossible to provide such a compact geometry due to the hodoscope's design. Therefore, the dependence of the shower's dimensions on the distance between the lead and the plane of the hodoscope's scintillators was measured (Fig.9). This dependence was extrapolated to a zero distance value in order to allow for non-compact geometry.

When estimating the showers' dimensions the following factors were taken into account:

1. The device's response function, calculated from the oscillograms obtained from single particles;

2. Correction for non-compact geometry;

3. Correction for non-linearity of the photomultiplier and the amplifier.

Figure 10a gives the dependences of the shower's dimensions on the lead thickness for various primary electron energies E =.5, 10, 14, 25 GeV. For comparison, we give a similar dependence obtained when the results given in Bathow's paper /10/ are applied to the conditions for measuring the showers' transverse dimensions

using a hodoscope (the cross-section distribution is obtained from the shower's radial distribution). Fig. 10b gives the dependence on the lead thickness of the standard deviations in the distributions of the showers' transverse dimensions for the energies E = 5 GeV and 14 GeV. The dimensions of showers in laminar media with lead plates 5 mm. thick equidistantly spaced along bases of 20 cm. and 40 cm. were defined in the shower's maximum development region for energies E = 2,5; 5; 10; 14 GeV. The results of these measurements are given in table 2.

Table 2

The statistical measurement errors do not exceed ± 10%.

E /GeV/	Thickness of lead layer/mm/	2τ /mm/	2τ /mm/ 20 cm	2τ /mm/ 40 cm
2,5	30	9	11,5	15
5	30	10,5	13,5	15
10	40	11		17
14	35	13	17	20

The insertion of plexiglass plates in the gaps between the lead plates had virtually no effect on the dimensions of the showers within the error limits.

In conclusion, the authors wish to thank Yu.D. Prokoshkin for his constant interest in the paper, N.K. Vishnevskij for his help with the measurements and A.M. Mestvirishvili for his assistance in the $1K^0$ channel operations.

Bibliography

1. K.N. Gubrienko, E.V. Eremenko, V.I. Kotov et al. IHEP Preprint 69-77, Serpukhov, 1969.

2. F. Binon, S.P. Denisov, P. Dyutejl' et al. IHEP Preprint 69-78, Serpukhov, 1969; Ya.F. 11, 3, 1970; Phys. Lett., 30B, 506, 1969.

3. A.I. Alikhanyan, L.S. Bagdasaryan, G.L. Bayatyan et al. IHEP Preprint 70-105, Serpukhov, 1970.

4. S.V. Donskov, V.A. Kachanov, V.M. Kut'in et al. IHEP Preprint 68-16-K, Serpukhov, 1968; PTE, 3, 60, 1969.

5. N.F. Alexandrova, N.K. Vishnevskij, O.S. Korol'kova et al. Preprint 69-22, Serpukhov, 1969.

6. A.F. Dunajtsev, Yu.I. Ivan'shin, D.B. Kakauridze et al. PTE. 1, 48, 1971.

7. C.A. Heuch. Proc. of Int. Symp. on Electron and Photon Inter. at High-Energies. Hamburg, 11, 408, 1965.

8. G. Backenstoss et al. Nucl. Inst. Meth., 21, 155, 1963.

9. B. Rossi. High-energy particles. HITTL, 1955, 338 pp.

10. G. Bathow et al. Preprint DESY 69/39, October 1969.

The document was received by the publishers on 20 September 1971.

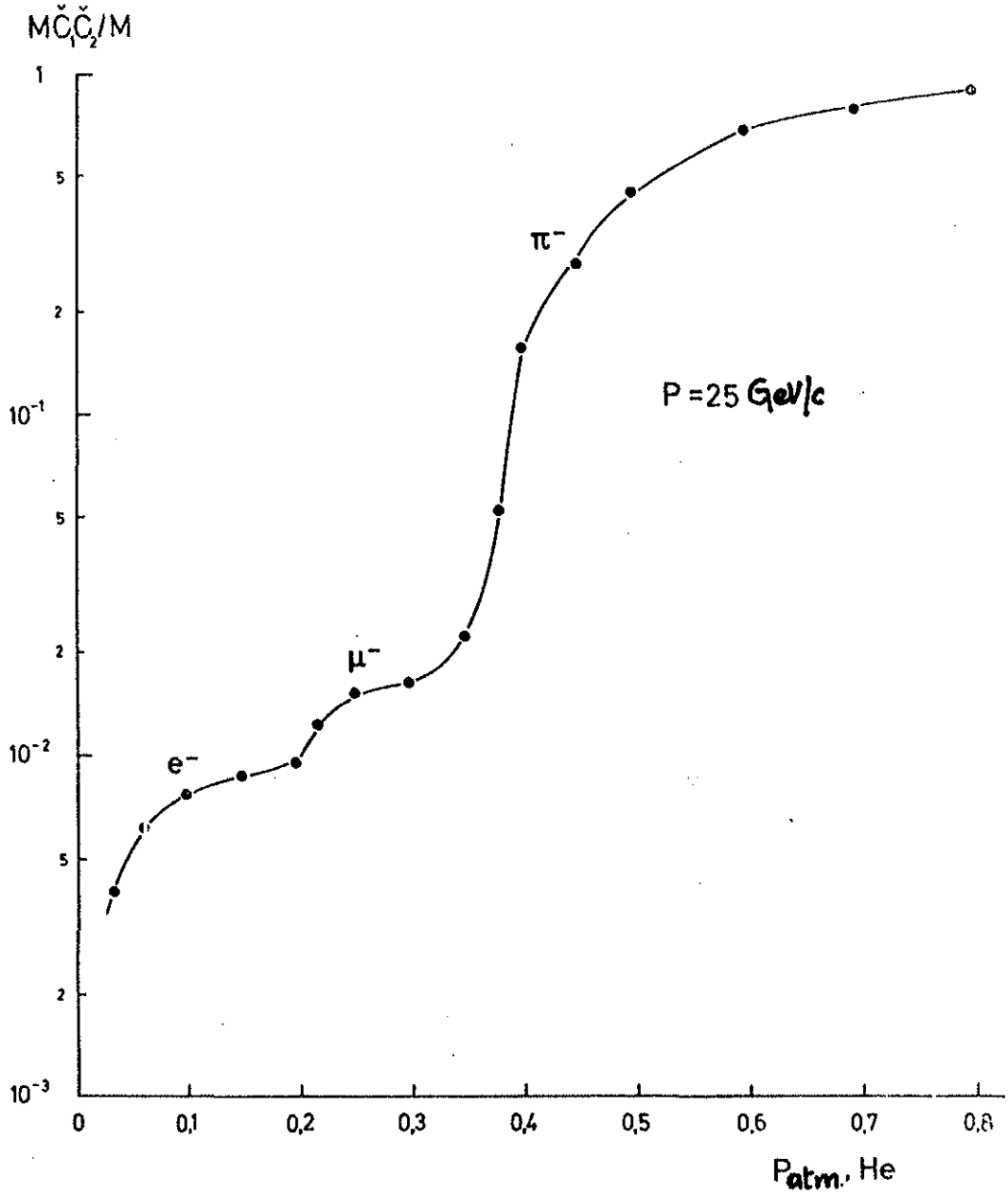

Fig. 1. Threshold curve for simultaneous variation of pressure in two Cerenkov counters.

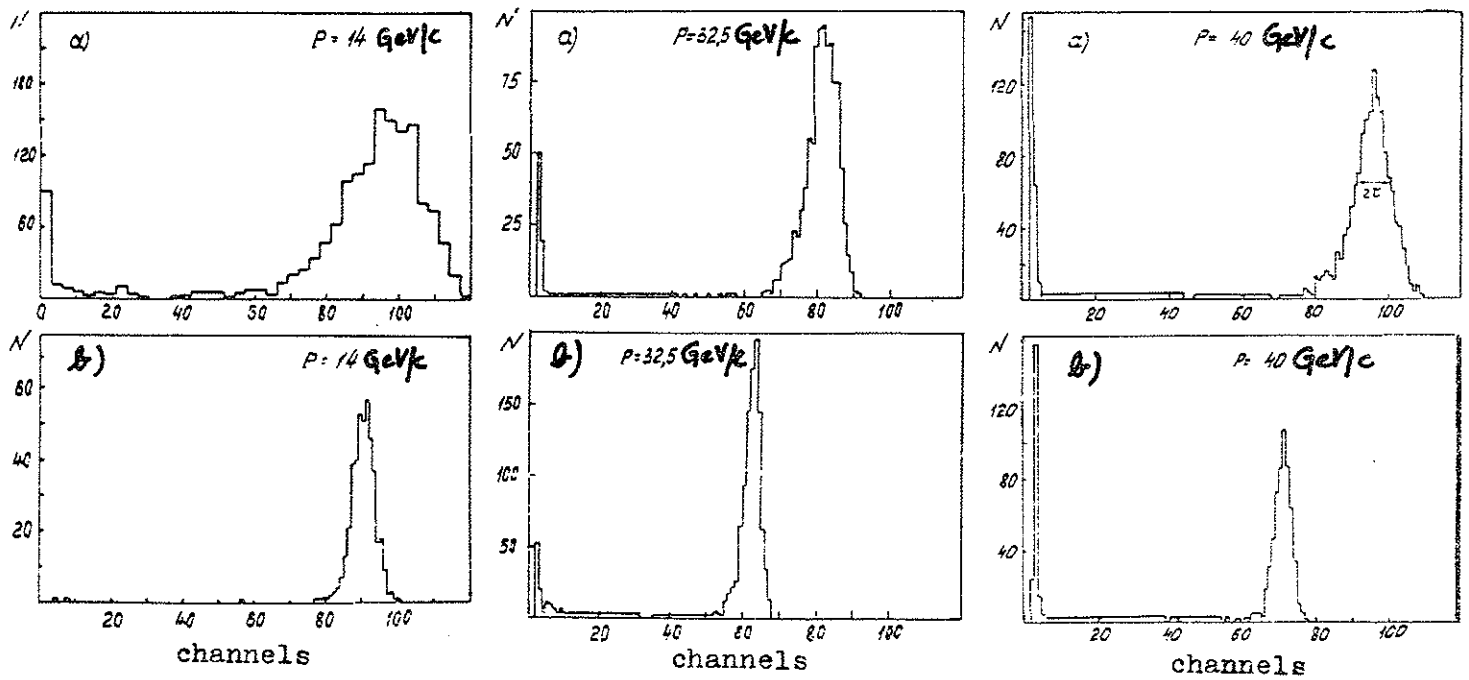

Fig. 2. Pulse-height spectra obtained when electrons of different energies are detected by means of the sandwich for measurements in the region of the shower curve maximum (a) and by means of a total absorption sandwich (b). Measurements at P = 14 GeV/c were carried out on the 1K° channel.

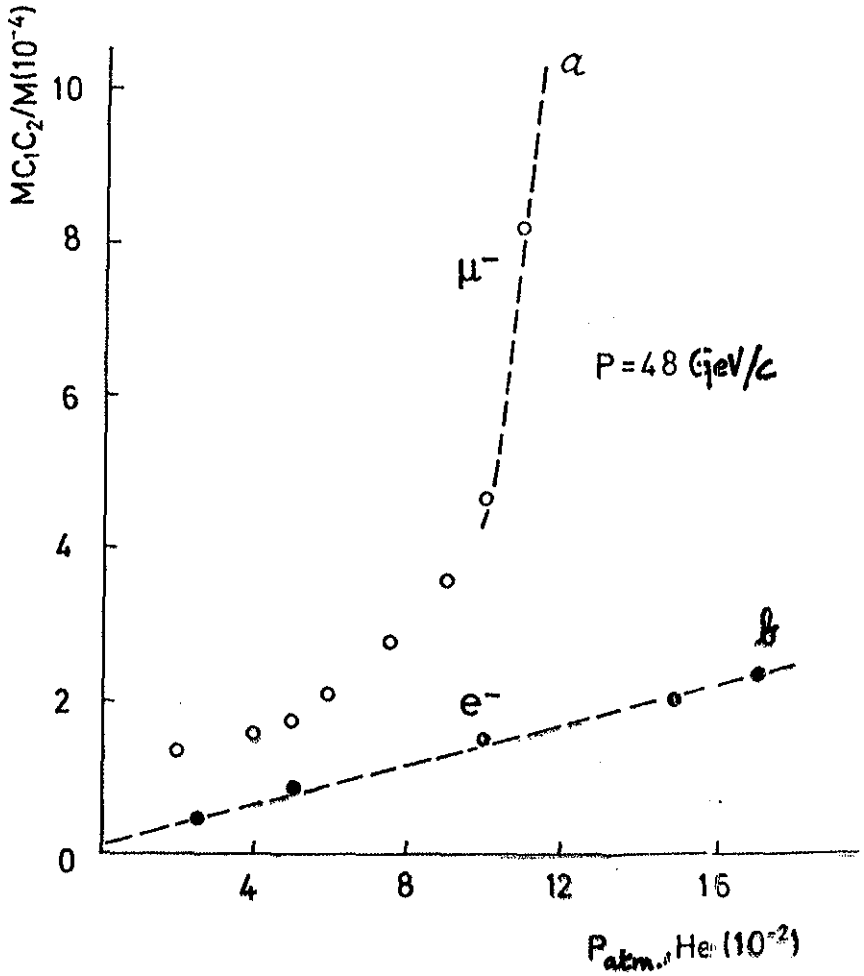

Fig. 3. a) Threshold curve for simultaneous variation of pressure in two Cerenkov counters.

b) Dependence of the count in the electron peak on the pressure in counters.

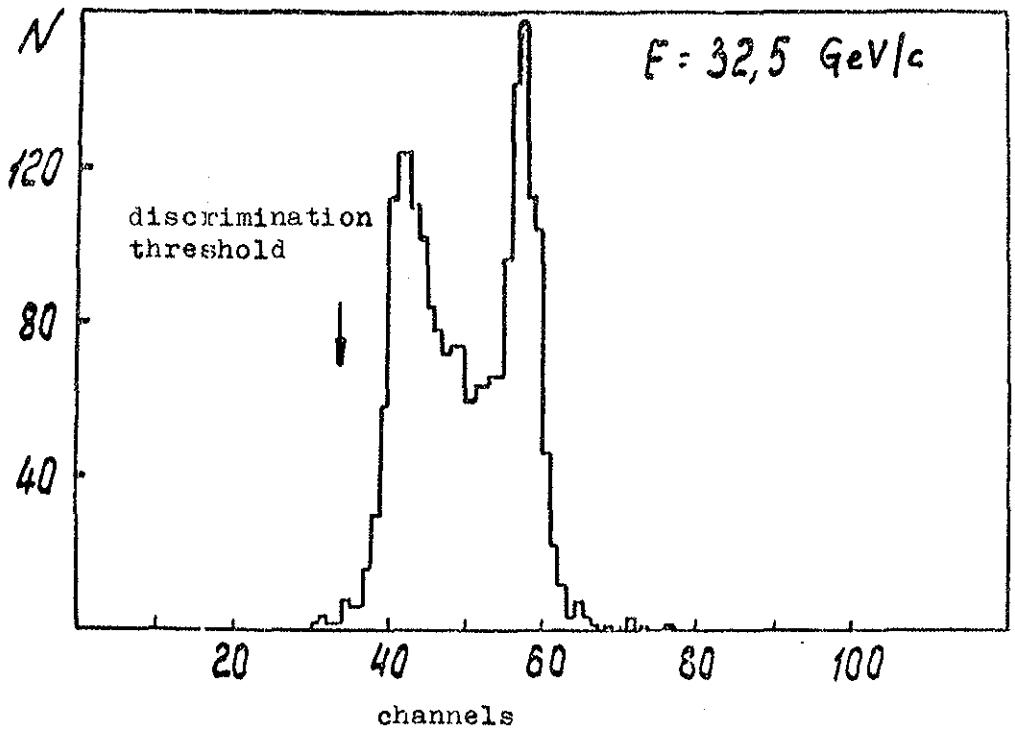

Fig. 4. Direct selection of electrons from the beam by means of the total absorption sandwich (not using threshold counters) P = 32,5 GeV/c. Discrimination was introduced in order to reduce the rate of the pulse-height analyzer.

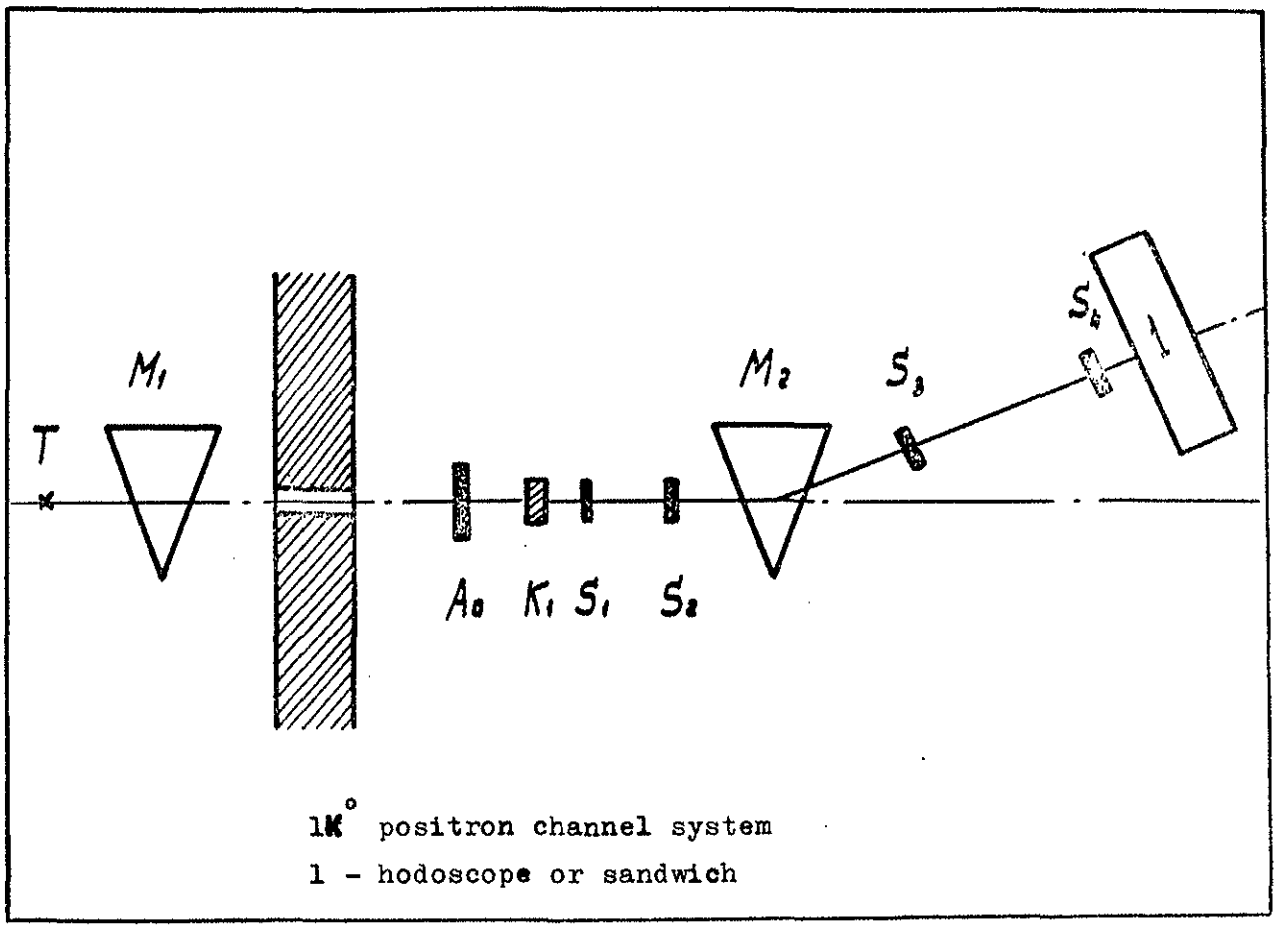

Fig. 5. System for selecting the electron beam in the 1K° channel: T - target, M_1 - clearing magnet, M_2 - pulsed magnet, K_1 - electron converter, S_1 - S_4 - telescope counters, A_0 - counter connected in anti-coincidence with the telescope.

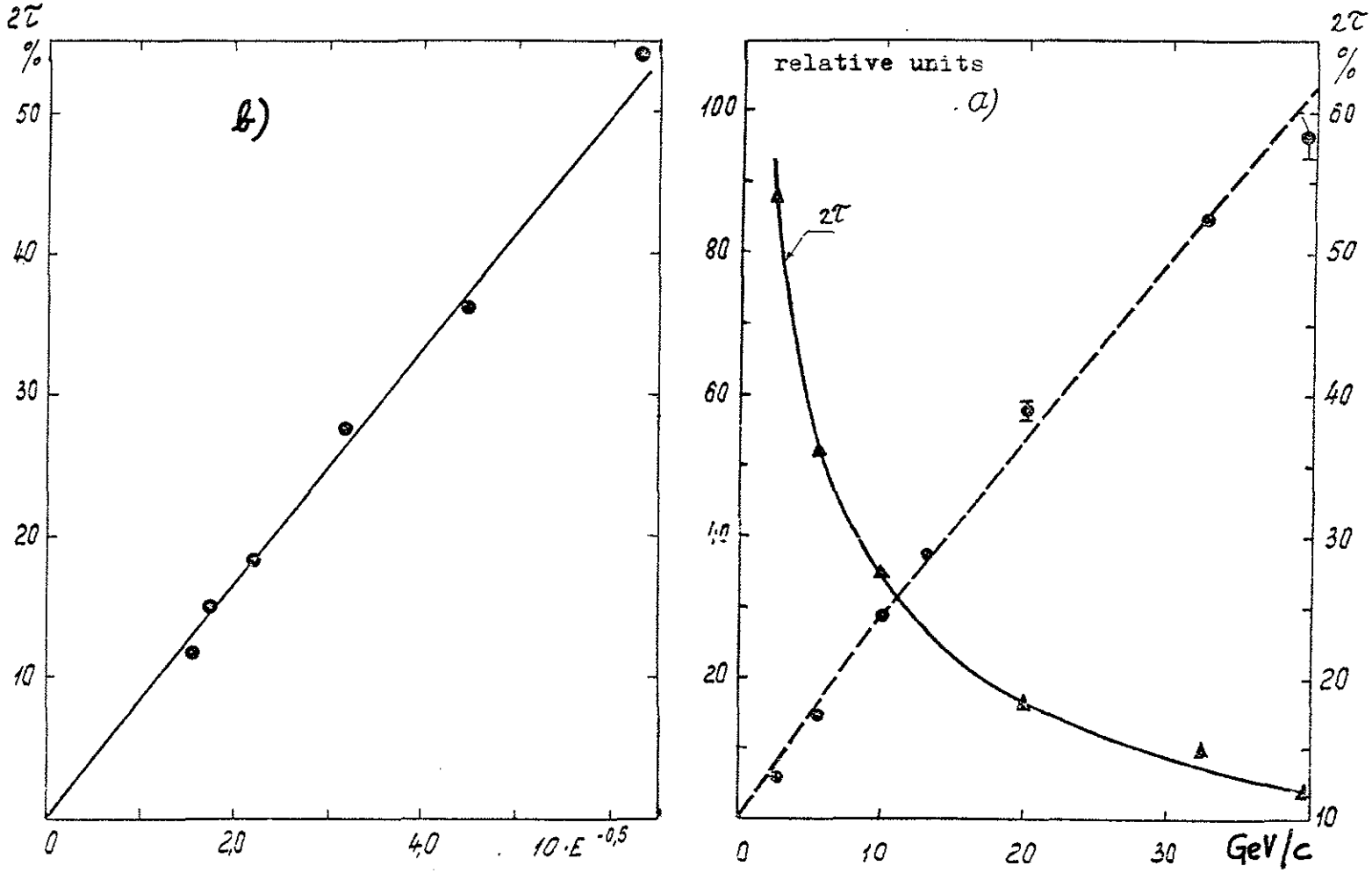

Fig. 6. a) Dependence on momentum of the energy resolution and mean values of the pulse height spectra of the sandwich (2,5 cm. Pb). The hatched line indicates dependence (1).

b) Dependence on momentum (within the coordinates $E^{-0,5}$, $GeV^{-0.5}$) of the energy resolution of the sandwich (2,5 cm. Pb).

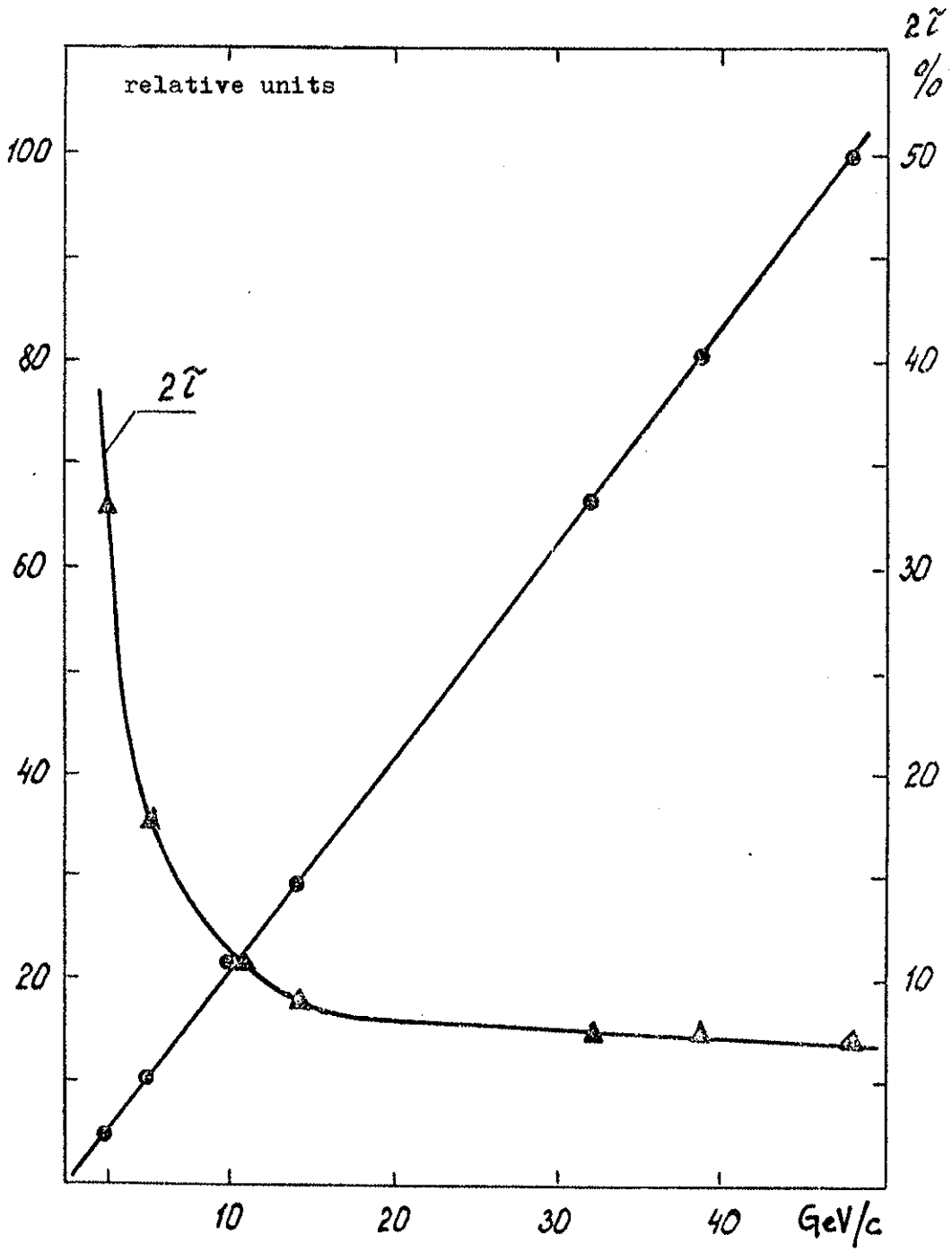

Fig. 7. Linearity and energy resolution of the total absorption sandwich.

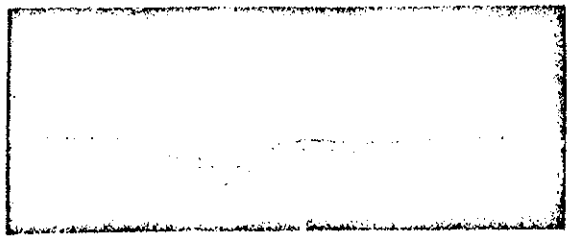

Fig. 8. Pulse oscillogram obtained by photographing hodoscope pulses on the oscilloscope screen when an electron shower in the region of the shower curve maximum is detected. The duration of the sweep is 500 nsec.

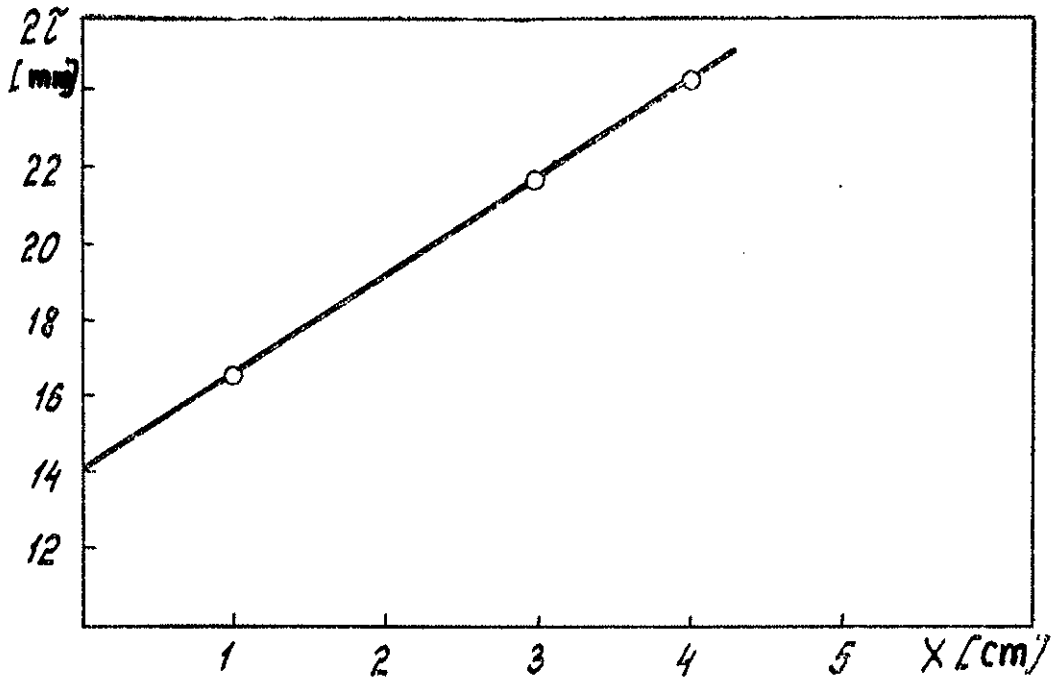

Fig. 9. Dependence of the shower's dimensions on the distance X between the lead and the plane of the scintillators.

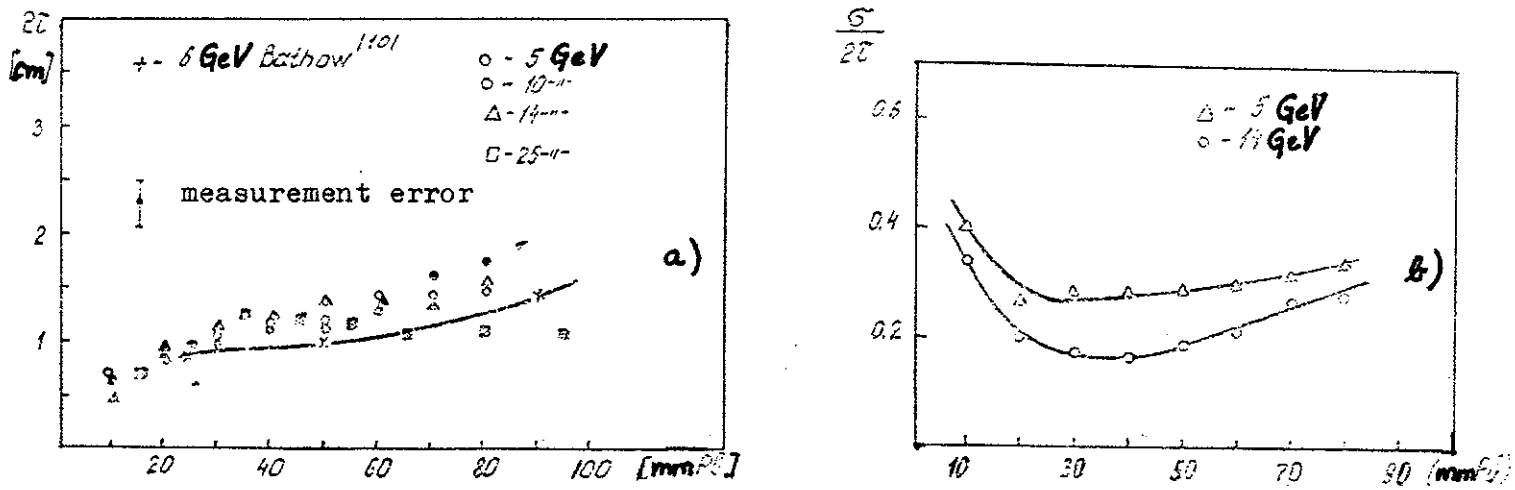

Fig. 10. a) Dependence of the shower's dimensions on the thickness of the lead for energies E = 5; 10; 14; 25 GeV.

b) Dependence on the lead's thickness of the standard deviations in the distributions of the electron showers' transverse dimensions.